

Coralgal buildup in a mixed carbonate-siliciclastic succession of the Upper Eocene Sant Martí Xic formation (Orís, Vic, SE Ebro basin, Spain)

Alessandro Mancini¹ Marco Brandano¹ Giovanni Gaglianone¹ Domenico Mannetta¹ Carles Ferràndez-Cañadell²

¹University of Rome "Sapienza", Department of Earth Sciences

Piazzale Aldo Moro, 5 00185, Rome, Italy. Mancini E-mail: a.mancini@uniroma1.it

²Universitat de Barcelona-UB, Faculty of Earth Sciences, Department of Earth and Ocean Dynamics

Carrer de Martí i Franquès, s/n, 08028, Barcelona, Spain

ABSTRACT

Coralgal buildups from the mixed carbonate siliciclastic succession of the upper Eocene Sant Martí Xic Formation (Orís, Vic, SE Ebro basin, Spain) were studied. During the upper Eocene, the sedimentation in the Orís area was strongly influenced by global and local factors associated with the evolution of the Ebro Basin. The stratigraphic series in Orís shows first a transgressive sedimentary sequence characterized by floatstone to rudstone limestone with *Discocyclus* and *Nummulites*, which developed in a deeper and oligophotic environment and in a general context of humid climate conditions. The second sequence is formed by progradational deltaic deposits rich in *Nummulites* and developed under more arid climate conditions. Coralgal buildups occur interdigitated with these deltaic deposits forming two different lens-shaped bioherms that resulted in a coalescent buildup, with coral colonies sparse in a skeletal matrix of different grain-size. Corals grew in the mesophotic zone of the deltaic system affected by light fluctuations during periods of low siliciclastic input. The coralgal buildups of Sant Martí Xic Formation were thus influenced both by climatic changes and by the local detrital input from a deltaic system, associated with the uplift of the Catalan Coastal Range, highlighting the resilience of Eocene corals to environmental change.

KEYWORDS Cluster reef. Mesophotic corals. Priabonian. Delta. Climate change.

INTRODUCTION

Priabonian coralgal buildups from the Ebro Basin (Spain) are represented by nodular limestone that crops out especially in the Igualada (La Tossa de Montbui; Salas, 1979) and Vic areas (Centelles, La Trona; Álvarez *et al.*, 1994, 1995, 1999; Barnolas *et al.*, 1983; Santisteban and Taberner, 1988). These beds are among the last marine deposits of the Ebro Basin (Costa *et al.*, 2013; Garcés *et al.*, 2020) and were previously interpreted as fringing reefs or coral mounds developed in a deltaic complex, under high

hydrodynamic conditions (Ferrer *et al.*, 1968; Santisteban and Taberner, 1988; Barnolas, 1992; Álvarez *et al.*, 1999; Taberner and Bosence, 1995). Several authors that studied coeval/similar successions characterized by the same lithofacies rich in coralgal buildups from the Southern central Pyrenees and Alpine Foreland Basin (Bosellini and Trevisani, 1992; Bosellini and Papazzoni, 2003; Nebelsick *et al.*, 2005; Rasser, 2009; Morsilli *et al.*, 2011; Pomar *et al.*, 2017), concluded that such hermatypic corals were developed under relatively high sedimentation rates, and associated to turbid water and in mesotrophic conditions. In

general, the Bartonian-Priabonian coral buildups represent one of the four major episodes of extensive coral buildup development during the Cenozoic (Pomar et al., 2017). These buildups were formed during global cooling phases, as evidenced by positive trends in $\delta^{18}\text{O}$ values, which also coincide with periods of reduced oceanic fertility reflected in lower $\delta^{13}\text{C}$ values. Pomar et al. (2017) highlight two distinct drops in the global temperature, which align well with two distinct key stages in the evolution of the symbiotic zooxanthellae. During the first Cenozoic interval, lasting until the Lutetian, coral buildups retained affinities with Cretaceous assemblages. The first significant cooling event occurred in the Bartonian-Priabonian transition and corresponded to the initial diversification of the *Symbiodinium* group of zooxanthellae (Pochon and Pawlowski, 2006). In addition, Bartonian-Priabonian corals often developed under mesophotic and high turbidity conditions (Taberner and Bosence, 1995; Morsilli et al., 2012; Pomar et al., 2017).

Recently, coral reefs exposed to high turbidity, reduced light penetration, and significant sediment input have attracted considerable scientific attention (see Zweifler et al., 2021 and Bosellini et al., 2024 for a review), challenging the long-held idea that clear, warm, and oligotrophic waters are essential for optimal coral reef growth. Evidence from modern oceans shows that turbid-water reefs may be more resilient to the impacts of climate change, particularly during prolonged periods of elevated sea-surface temperatures leading to severe bleaching events (Morgan et al., 2017; Sully and van Woesik, 2020; Rosedy et al., 2023; Bosellini et al., 2024). As a result, this type of reefs was positioned as a potential ecological refugium (Beger et al., 2014). In the geological record, many coral reefs and coral assemblages are found in association with marly and mixed carbonate-siliciclastic sediments (Wilson and Lokier, 2002; Sanders and Baron-Szabo, 2005; Morsilli et al., 2011; Santodomingo et al., 2015, 2016; Pomar et al., 2017; Reuter et al., 2019; Woolfe and Larcombe, 1998; Perry and Smithers, 2006; Lesser et al., 2009; Tomassetti et al., 2013; Bosellini et al., 2024), often related to deltaic systems (Lokier et al., 2009; Morsilli et al., 2011). Thus, the development of coral buildups is clearly influenced by a combination of global and local factors. In this study, we aim to disentangle the contributions of these various influences, with a particular focus on the climatic conditions that governed terrigenous input.

GEOLOGICAL SETTING

The investigated area (Orís) is located in the eastern margin of the Ebro Basin (Spain) and shows autochthonous deposits extending from the Vic area in the west to the Camós-Celrà extensional fault to the east (Saula et al.,

1994). To the north, the study area is bounded by the South Pyrenean frontal thrust (Muñoz et al., 1986). From the Paleocene to the late Eocene the Ebro basin and the Vic area recorded sedimentation mostly in marine environments, as a result of subsidence related to the collision of Iberia with the European plate (Vergès et al., 2002) (Fig. 1). During this period, the Ebro Basin was connected to the Atlantic Ocean. Subsequently, reduced marine connection led to the deposition of evaporites in two different depocenters: the Catalan Basin to the east and the Navarra Basin to the west, separated by the central-southern Pyrenees thrust system. After the closure of the basin in the uppermost Eocene, the sedimentation evolved into alluvial-lacustrine sediments in the basin and conglomeratic sediments near the range margins (Garcés et al., 2020). The studied succession represents the final evolution of marine sedimentation in the autochthonous part of the southern Pyrenees foreland basin.

From the early Eocene to the Oligocene, the south-eastern margin of the Ebro Basin was strongly influenced by the uplift of the Catalan Coastal Range thrust. The central part of this zone shows the most pronounced deformation, which took place from the middle to late Eocene accompanied by the syn-sedimentary evolution of deltaic systems (Cabello et al., 2010; López-Blanco et al., 2000). These deposits gradually evolved into basinal sedimentation with shallow marine limestones and clastic sediments (e.g. in the Igualada area, Serra-Kiel et al., 2003a, b).

From the stratigraphic viewpoint the study area (Orís) shows a complete Priabonian succession (Fig. 1) formed by two sedimentary sequences (Costa et al., 2013; Sanjuan et al., 2012; Serra-Kiel et al., 1998, 2003a, b). The first one was a transgressive sequence, with a maximum flooding surface represented locally by bryozoans and *Discocyclus* marls that developed in a deep and oligophotic environment (Serra-Kiel et al., 2003a), while the subsequent regressive sequence shows instead coralgal facies of the Sant Martí Xic Formation interdigitated with progradational deltaic sediments (*Upper deltaic reefal complex* in Serra-Kiel et al., 2003b). These deposits were covered by the Terminal Complex carbonates defined by Travé et al. (1996) that evolved into the transitional and non-marine sediments of the Sant Boi de Lluçanès and Artés formations (Sanjuan et al., 2012). This transition corresponds to the last marine event of the eastern Ebro Basin.

MATERIAL AND METHODS

Seven stratigraphic logs were studied, with logs 1, 2, 3, 5 and 7 representing the lateral part of the coralgal buildups, while logs 4 and 6 represent their central part. A detailed by sedimentological analysis and lithofacies characterization was performed. The stratigraphic logs, ranging 65–70m in

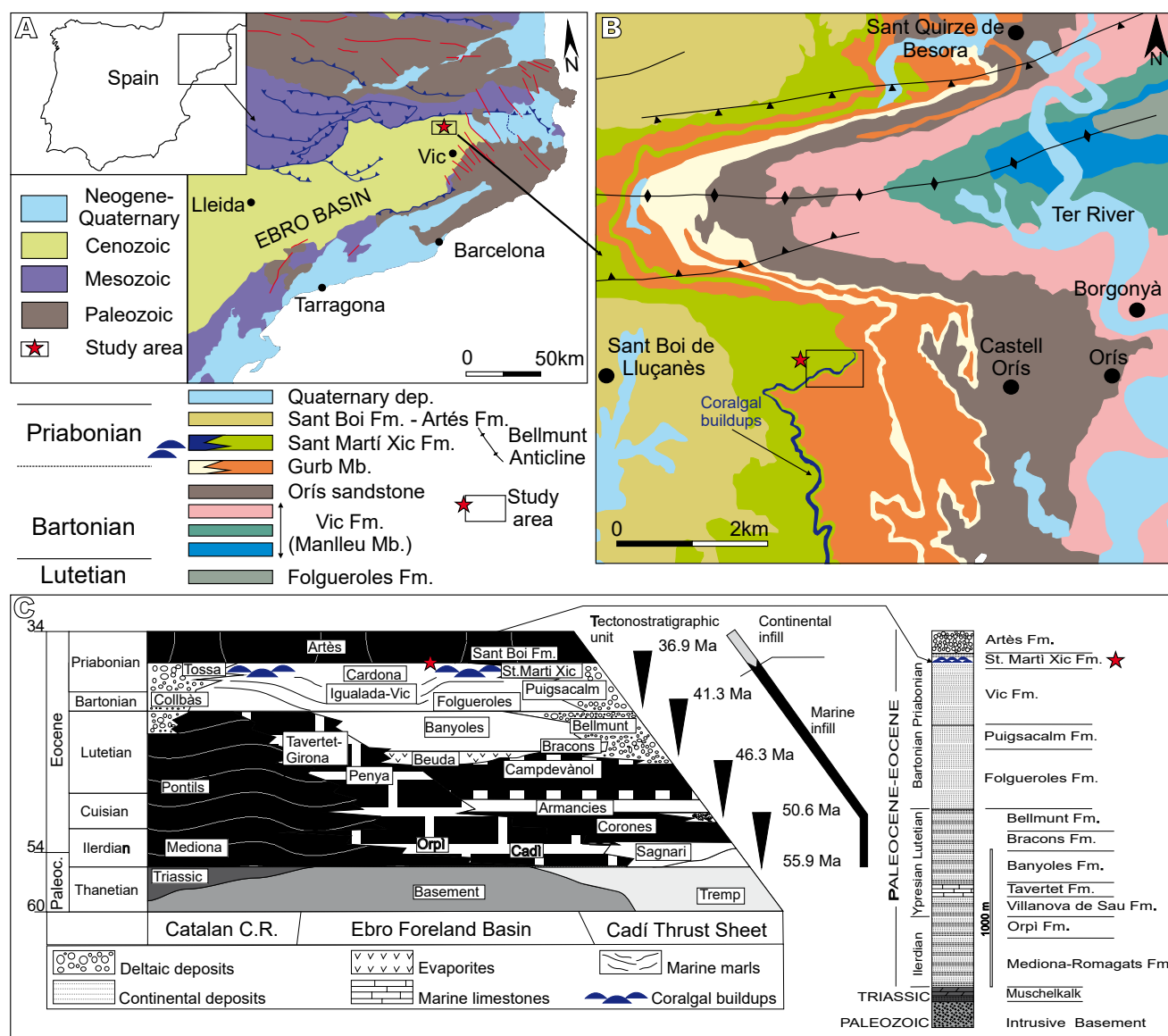


FIGURE 1. Geological setting of the study area. A) Geological map of the eastern Ebro Basin. B) Geological map of the study area. C) Stratigraphic units of the Ebro Basin, showing the lateral relationships from the Catalan Coastal Range to the Cadí thrust sheet, the tectonostratigraphic units, and the change from marine to continental sedimentation (modified from Vergés et al., 2003; Sanjuan and Martín-Closas, 2012).

thickness (Fig. 2), were measured in the Orís hill, located at Serrat dels Bous hills near Sant Salvador de Bellver church (18.8km north of Vic). Microfacies analysis, texture characterization and identification of skeletal components was based on the study of 40 thin section, following the texture classification given in Dunham (1962) and Insalaco (1998). Carbonate content was measured to evaluate the terrigenous percentage of the different lithofacies analysed. Up to 21 samples for the determination of the CaCO_3 fraction were collected. A weighted amount (some grams) of each sample was dissolved in a 5M HCl solution. Each solution was filtered with a cellulose acetate 0.45mm membrane filters and the insoluble residue was dried and weighted. The carbonate fraction of each sample has been computed from:

$$f\text{CaCO}_3 = (W_i - W_r)/W_i$$

where W_i is the initial weight and W_r the weight of the insoluble fraction.

RESULTS

Lithofacies

The studied succession, detailed in seven stratigraphic logs, was divided in six lithofacies, which are reported below from base to top. They characterize two sedimentary sequences, divided in stratigraphic intervals (Fig. 2;

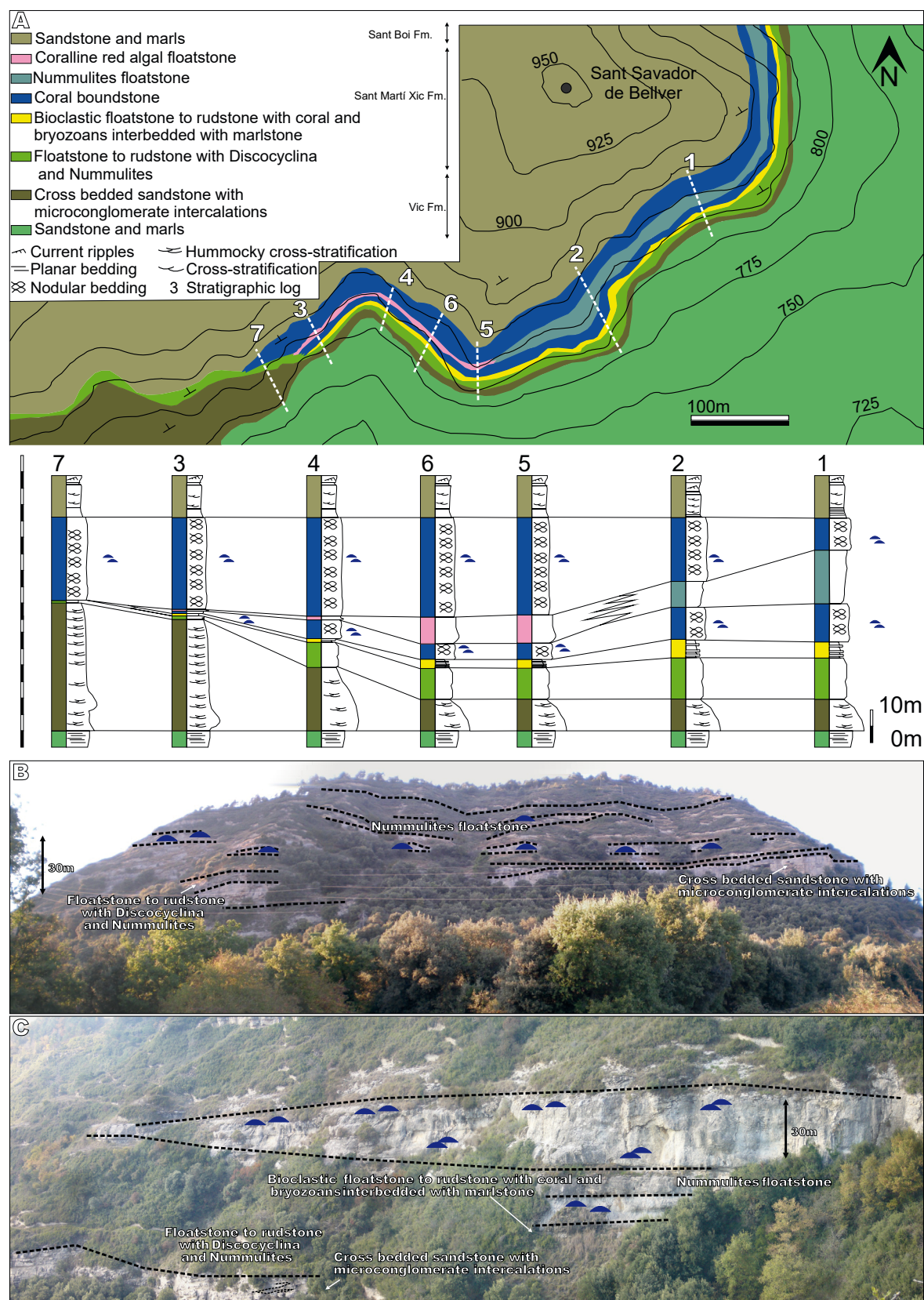


FIGURE 2. Stratigraphic setting of the study area. A) Detailed geological map with location of stratigraphic logs and their correlation. B-C) Panoramic view of the study area showing the geometries of the stratigraphic interval studied (stratigraphic profile). The blue shapes indicate the coralgal buildups.

3). The boundaries between the different stratigraphic intervals are characterized by vertical abrupt changes in lithofacies associated to non-planar contact surfaces with important thickness variations (see also Fig. 2). The only lateral heteropic change observable in the study area is represented by the *Nummulites* and coralline red algal floatstone lithofacies.

Cross bedded sandstone with microconglomerate intercalations

This lithofacies, 5–10m thick, is characterized by yellow fine sandstone with intercalation of microconglomerate beds several decimetres thick. The sediment shows a variable amount of quartz. Other undetermined components are well-rounded. Hummocky cross-stratification occurred especially at the top of the level (Fig. 3A).

Floatstone to rudstone with *Discocyclus* and *Nummulites*

This lithofacies forms a grey lens-shaped interval, 0.5–13m thick, which develops on top of the cross-bedded sandstone with microconglomerate intercalations (Fig. 3B). Bed thickness varies between 1.5–10m, being sometimes difficult to observe due to amalgamation, especially in the thickest part of the interval. The CaCO₃ content amounts 98%. Bioclastic floatstone to rudstone (Fig. 4A) is characterized by the main occurrence of *Discocyclus* sp. and sparse *Nummulites* (*N. incrassatus* DE LA HARPE, *N. ex. gr. fabianii* (PREVER in Fabiani), and *N. ex. gr. striatus* BRUGUIÈRE, *Assilina* sp. and abundant fragments of echinoids, bryozoans and bivalves (oysters). The presence of *N. incrassatus* indicates a Bartonian-Priabonian age and the shallow benthic zones SB 17-18 of Serra-Kiel et al. (2003a). Vertical and horizontal bioturbation is common.

Bioclastic floatstone to rudstone with coral and bryozoans interbedded with marlstone

This interval, 0.5–5m thick, is characterized by alternating grey marlstone and nodular limestone (78% of CaCO₃ content), organized in tabular beds, 0.10–0.30m thick (Fig. 3C). Grey marlstone is laminated or structureless. The nodular limestone intervals are instead characterized by bioclastic floatstone to rudstone (Fig. 4B) with bryozoans, coralline red algae, fragments of bivalves (oysters), foraminifera (miliolids, *Gypsina moussaviani* BRUGNATTI & UNGARO, *Fabiania cassis* OPPENHEIM, *Haddonella heissigi* HAGN, *Asterigerina rotula* (Kaufmann), *Gyroidinella magna* LE CALVEZ, rare *Nummulites ex. gr. fabianii* and corals. Coral fragments are bioeroded by sponges (*Entobia* ichsp.) and bivalves (*Gastrochaenolites* ichsp.) and encrusted by coralline red algae and serpulids and sometimes are completely re-crystallized.

Coral boundstone

Coral boundstone lithofacies (Fig. 3C, D) forms two different lens-shaped intervals separated by *Nummulites* and coralline red algal floatstone (see description below). Coral colonies are sparse in a skeletal matrix characterized by different lithofacies (Fig. 4C, D; Fig. 5A-L). Grainstone with fragments of intensively bioeroded corals, coralline red algae, *Nummulites ex. gr. fabianii*, *Gypsina moussaviani* and miliolids, characterizes the central part of the interval (Fig. 5E-F), while rudstone to packstone/wackestone and baffestone (Fig. 5A, B, C, D, G, H, I, J, K, L) with corals encrusted by *Fabiania cassis*, coralline red algae, miliolids, rhodoliths, *Nummulites* (*N. ex. gr. fabianii*, *N. ex. gr. striatus*), gastropods, *G. moussaviani*, victoriellids, gastropods, serpulids, rare fragments of bryozoans, oysters and intraclasts characterizes instead the marginal part. The thickness of the first interval varies 1–7m, while the second is up to 32m thick. The first coral interval is not well-organised laterally and vertically, whereas the second one is highly organised with larger coral colonies. The colonies show different growth patterns (branching, thick-branched, phaceloid, rare platy and dome) organised in a “mixstone” (*sensu* INSALACO, 1998). Relatively few coral taxa are present in either layer: *Cereiphylla*, *Ellipsocoenia*, *Goniopora*, *Caulastrea* and *Actinacis* (Fig. 6A, B, C, D). The largest colonies are 55–80cm (mean 26.8cm) in diameter and 14–25cm (mean 12.8cm) high. Corals are fragmented and abraded, whereas bioerosion values are variable, with higher values in logs 1 and 7, which correspond to marginal parts of the intervals. The bioerosion corresponds to sponges (*Entobia* ichsp.) and bivalves (*Gastrochaenolites* ichsp.) and several colonies are encrusted by coralline red algae and foraminifera (*Solenomeris*). Secondary processes are related to diagenesis and neomorphism (substitution of aragonite by calcite). In the Orís colonies, these processes are invasive and principally affect the *Actinacis* colonies, entirely replacing the internal structure and preserving only the exterior shape. The CaCO₃ content varies between 78% in the lower part of the intervals, to 98% in the upper part.

Nummulites floatstone

This lithofacies (Fig. 3E) separates the two coralgal buildups described above. It displays a variable thickness from 8m in the central part of the coral boundstone to 17.5m in its marginal part. Beds show planar stratification and sometimes are completely amalgamated. CaCO₃ content amounts 87%. Occasional bioturbations are observed in the lower part of the beds, while thin strata of microconglomerates may occur in the upper part. The poorly sorted floatstone (Fig. 4E) is dominated by *Nummulites* (*N. ex. gr. fabianii*, *N. ex. gr. striatus*, *N. ex. gr. incrassatus*), *G. moussaviani*, *Assilina schwageri* (SILVESTRI), *Assilina alpina* (H. DOUVILLÉ), *Asterigerina*



FIGURE 3. Lithofacies and outcrops of the study area. A) Cross-bedded sandstone with microconglomerate intercalations. B) Floatstone to rudstone with *Discocyclus* and *Nummulites*. C) Contact between the bioclastic floatstone-rudstone with corals and bryozoans interbedded with marlstone, and the first interval of coral boundstone. D) Contact between the coralline red algal floatstone and the second coral boundstone interval. E) Outcrop showing the characteristics of the *Nummulites* floatstone lithofacies. F) Outcrop view of coralline red algal floatstone.

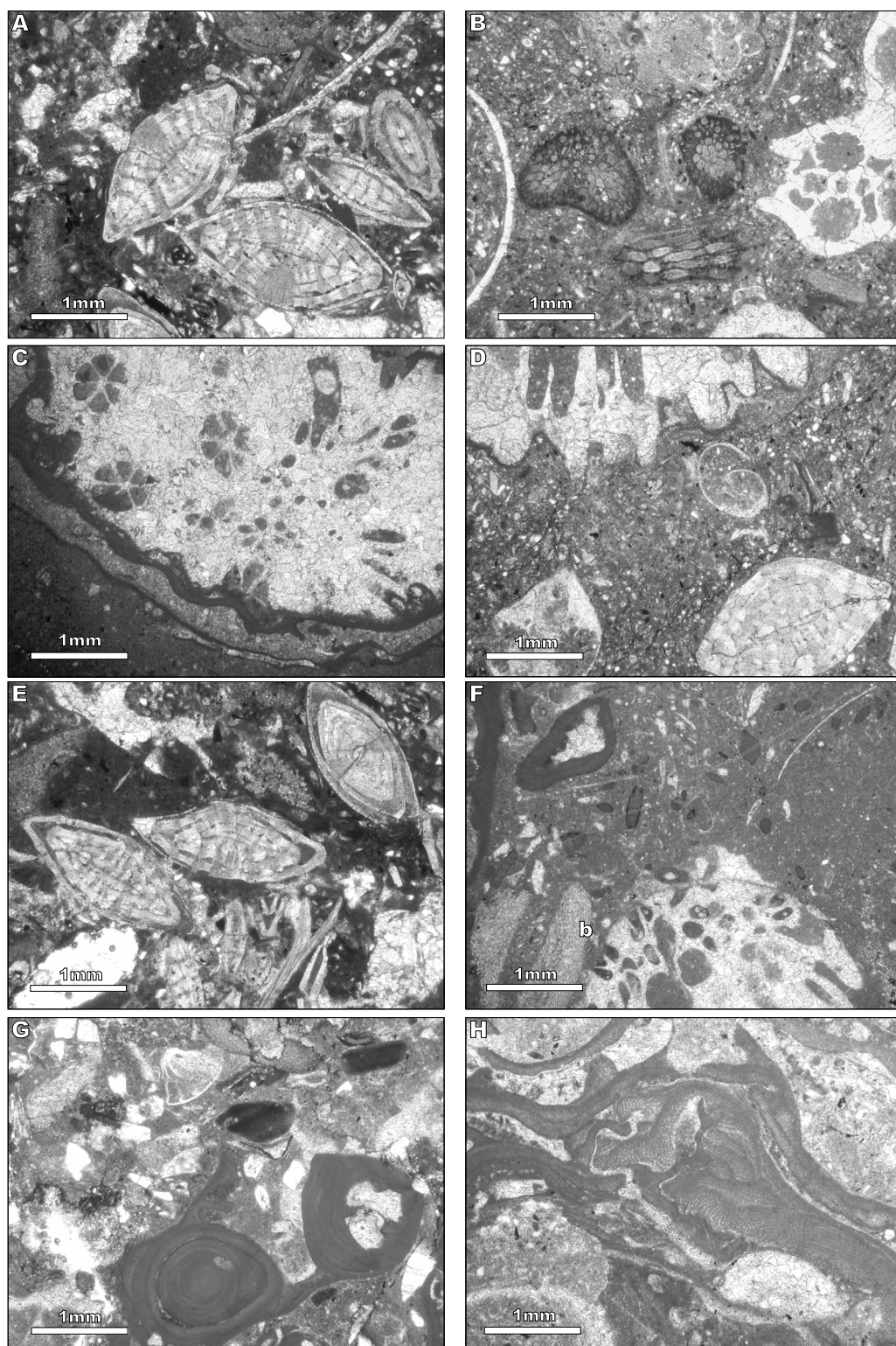


FIGURE 4. Microfacies of the lithofacies studied. A) Bioclastic floatstone with *Nummulites* and bivalve fragments from “Floatstone to rudstone with *Discocyclus* and *Nummulites* lithofacies”; B) Bioclastic rudstone with bryozoans from “Floatstone to rudstone with coral and bryozoans interbedded with marlstone lithofacies”; C) Bioeroded coral fragment encrusted by coralline red algae from “Coral boundstone lithofacies”; D) Bioclastic floatstone with coral fragments and *Nummulites* (*N. ex. gr. fabianii*) from “Coral boundstone lithofacies”; E) Floatstone with *Nummulites* (*N. incrassatus* and *N. ex. gr. fabianii*) from “Floatstone with *Nummulites* lithofacies”; F-G) Bioclastic floatstone with coralline red algae and bioeroded coral fragments from “Coralline red algal floatstone lithofacies”. To note the variability in the growth type of the coralline red algae (branching, encrusting or nodular) and the presence of *Gypsina moussaviani* (b in subfigure F), indicating a vegetated seafloor; H) Coralline red algal bindstone encrusting unidentified bioclasts from “Coralline red algal floatstone lithofacies”.

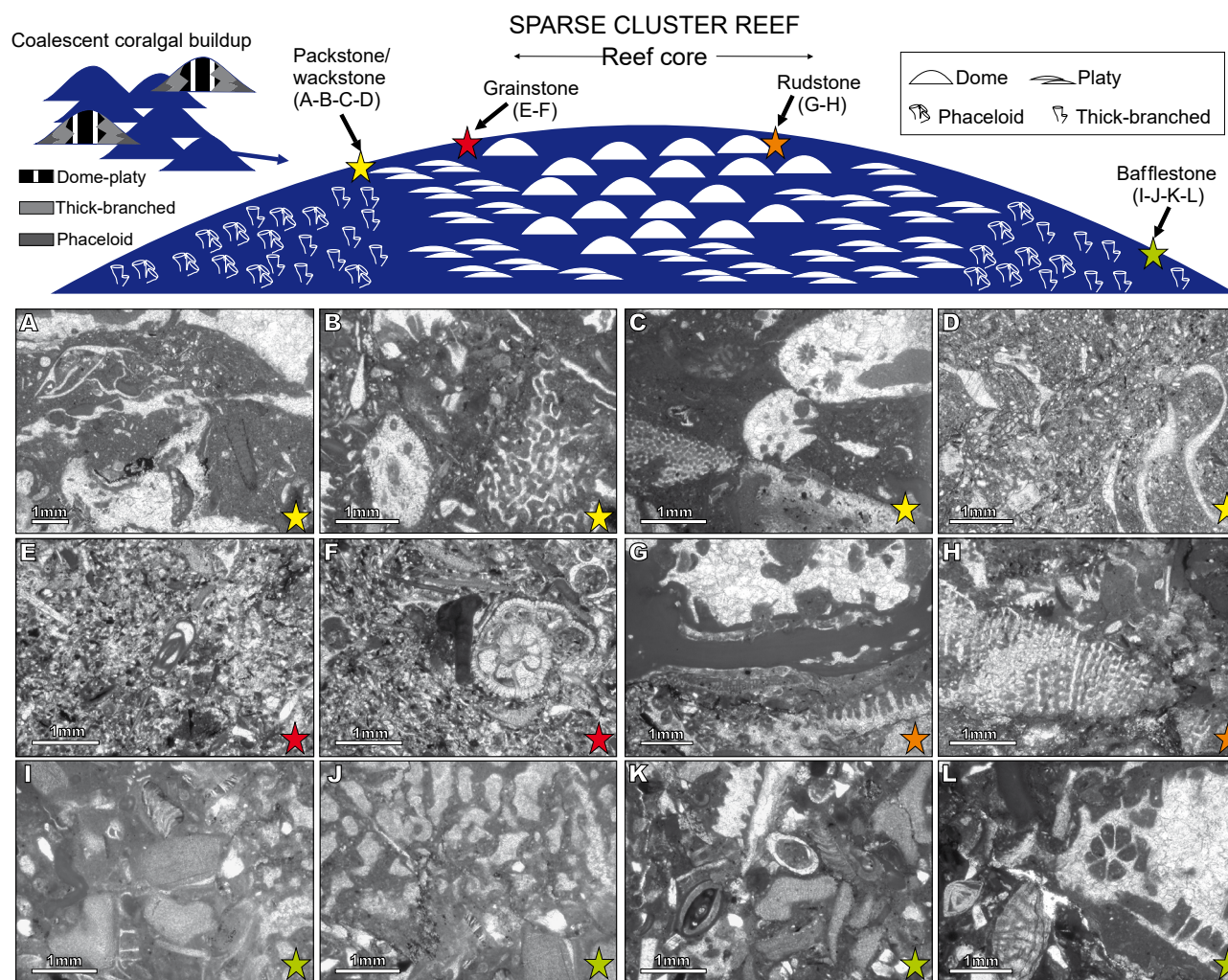


FIGURE 5. Distribution of the matrix fabrics in coral boundstone lithofacies. The coralgal buildups form two different lithosomes, which are characterized by small lens-shaped bioherms organized in a coalescent buildup, which develops on top of previous reliefs, maintaining the same distribution of coral growth-forms in each interval. A) Bioclastic packstone to wackestone with coral fragments, *Gypsina moussaviani*, bryozoans and coralline red algae; B-C) Wackestone with coralline red algae, bryozoans, miliolids, fragments of bivalves and bioeroded coral; D) Packstone to wackestone with fragments of bioeroded and encrusted corals (*Fabiania cassis*), bryozoans, fragments of gastropods, coralline red algae, *Nummulites ptukhiani-fabiani*, quartz and serpulids; E) Grainstone with fragments of corals, *Nummulites ptukhiani-fabiani*, miliolids, coralline red algae and *Gypsina moussaviani*; F) Grainstone with fragments of corals, coralline red algae, gastropods, *Nummulites* sp., *Gypsina* sp., cibicides, serpulids and *Gyroidinella magna*; G-H) Rudstone with fragments of corals encrusted by *Fabiania cassis*; I-J-K-L) Bafflestone with fragments of bioeroded corals, gastropods, serpulids, miliolids, coralline red algae and *Gypsina moussaviani*.

rotula (KAUFMANN), miliolids, fragments of coralline red algae, bivalves, and gastropods (*Campanile* sp.).

Coralline red algal floatstone

This lithofacies displays a lenticular geometry and is characterized by a variable thickness of 0.5–8m, replacing laterally the *Nummulites* floatstone (Fig. 3F). The tabular beds are characterized by floatstone (rare bindstone) fabrics with abundant coralline red algae and *Nummulites* (Fig. 4F, G, H). CaCO_3 content amounts 97%. Coralline red algae vary from encrusting to branched. Crusts were principally built on bioclasts of corals and molluscs, while branches may

be thick (up to 2cm long), to thin. The skeletal components include *Asterigerina rotula*, *Fabiania cassis*, epiphytic foraminifera such as *Planorbulina bronnimanni* BIGNOT & DECROUEZ and *Gypsina moussaviani* (Fig. 4F), miliolids, vermetids, rare encrusting bryozoans and fragments of corals, sometimes bioeroded (*Entobia* ichsp.).

DEPOSITIONAL MODEL

Facies analysis performed on the two sedimentary sequences of the Orís succession allows reconstructing the evolution of depositional settings passing from a lower

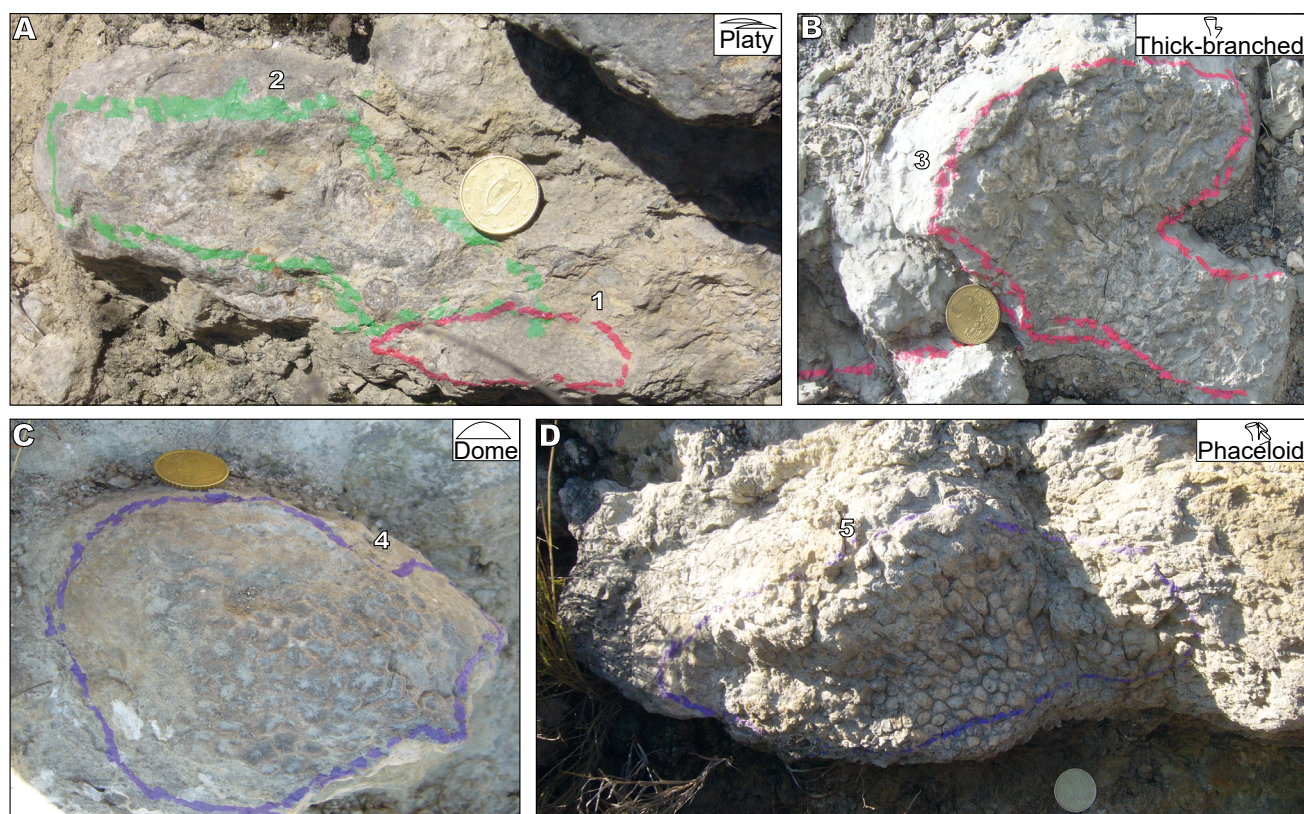


FIGURE 6. Growth types of coral colonies; A) Platy; B) Thick-branched; C) Dome; D) Phaceloid. Legend: 1= *Goniopora* sp.; 2-3= *Actinacis* sp.; 4= *Ellipsocoenia* sp.; 5= *Cereiphylla* sp.

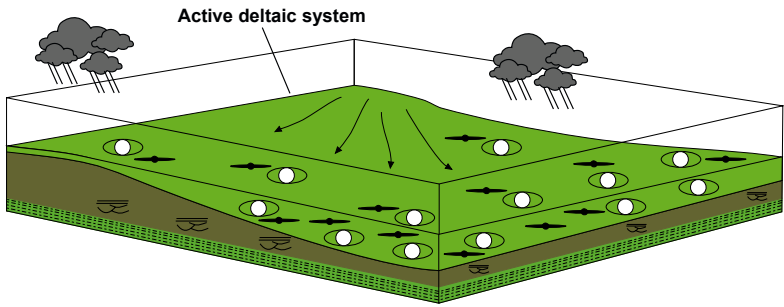
transgressive sequence (Fig. 7, stages 1-2) to the upper regressive sequence (Fig. 7, stages 3-5), as also reported by Serra-Kiel et al. (2003a, b). In particular, the lithofacies observed on the lower part of the succession (Fig. 7, stage 1) attests for a depositional environment mainly associated to pro-delta (Ferrer, 1971), sometimes affected by episodic high energy events related to the activity of the delta front system and testified by the cross bedded sandstone with microconglomerate intercalations. Above previous facies, rudstone to floatstone with *Discocyclus* and *Nummulites* suggests deposition in a deeper environment (Fig. 7, stage 1), probably below the fair-weather wave-base level. In particular, *Discocyclus* is usually interpreted as inhabiting deeper water (outer ramp or lower photic zone (e.g. Beavington-Penney and Racey 2004; Romero et al., 2002), since it is commonly associated to marls and shows morphological adaptations to low light intensity (e.g. Ferrández-Cañadell and Serra-Kiel, 1992; Romero et al., 2002). The absence of tractive structures excludes transport and accumulation of these larger foraminifera under the action of sea-bottom currents. Analogous facies, with similar foraminiferal assemblages, have been also described in the Alpine foreland basin (e.g. the “nummulitid and orthophragminid” biofacies of Coletti et al., 2021), in the Eocene Foraminiferal Limestone of Pag (Croatia; Mariani

et al., 2024), and in the upper Eocene Nago limestone, Trento, Northern Italy (Bassi, 1998). The lack of shallow-water skeletal biota indicates minimal reworking processes, supporting the conclusion that the components were autochthonous in the depositional setting.

Bioclastic floatstone to rudstone with corals and bryozoans and marlstone deposited above the rudstone to floatstone with *Discocyclus* and *Nummulites*, suggest a transgression and a change in the hydrodynamic conditions to a low energy environment (Fig. 7, stage 2), as also reported in Barnolas et al. (1988) and Serra-Kiel et al. (2003a). The coral boundstone lithofacies developed in this deltaic complex and on top of the floatstone to rudstone with coral and bryozoans interbedded with marlstone (Fig. 7, stage 2) is associated to deposition below the wave-base level in a prodelta setting. A similar situation was described in the Ainsa Basin, in the South-Central Pyrenean zone (Morsilli et al., 2011). The coralgal buildups form two different lithosomes with the same texture and lithofacies. In particular, corals develop into small, lens-shaped bioherms organized in a coalescent buildup (Fig. 5). This larger buildup grew on top of previous reliefs with the grainstone facies occupying the central part of the reef core (Fig. 5E, F), the packstone-wackestone facies placed

First stage

- Humid climatic conditions.
- Deposition below wave-base.
- Low light intensity due to water turbidity (active deltaic system).
- Intermediate ramp.

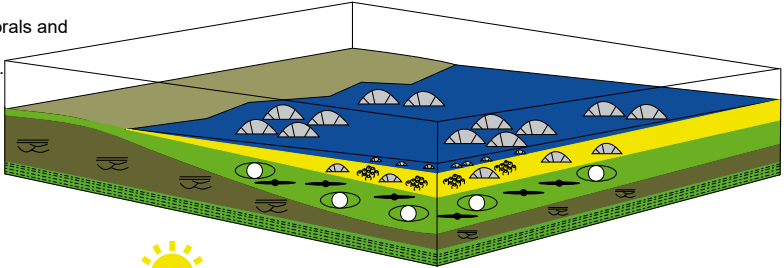


Second stage

- Bioclastic floatstone to rudstone with corals and bryozoans interbedded with marlstone:
- Change in the hydrodynamic condition.
 - Onset of a low energy environment.
 - Low sediment supply

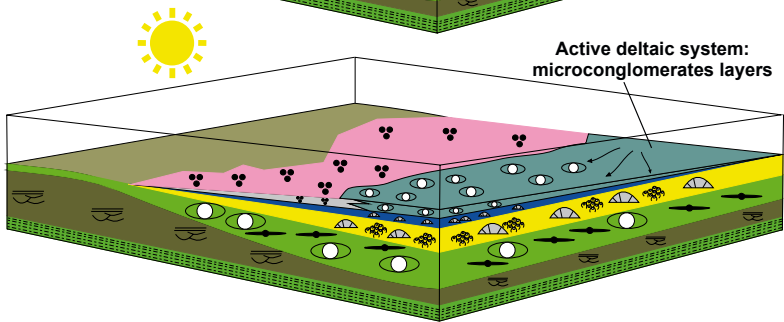
Coral boundstone:

- Depositional environment below the wave-base under limited deltaic activity.



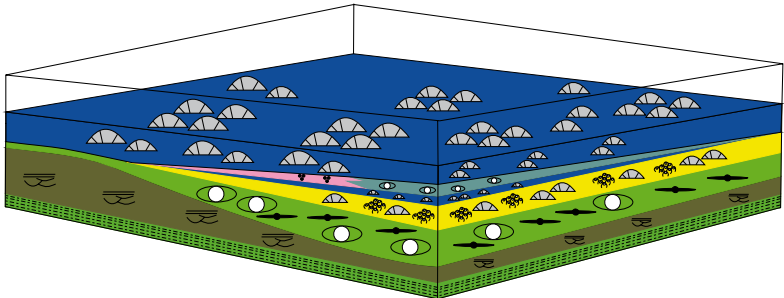
Third stage

- Dry climatic conditions.
- Depositional environment affected by the activity of the deltaic system (Floatstone with Nummulites).
- Seagrass, developed during period without the activity of delta fan and relatively low turbidity or far from the activity of the deltaic system.



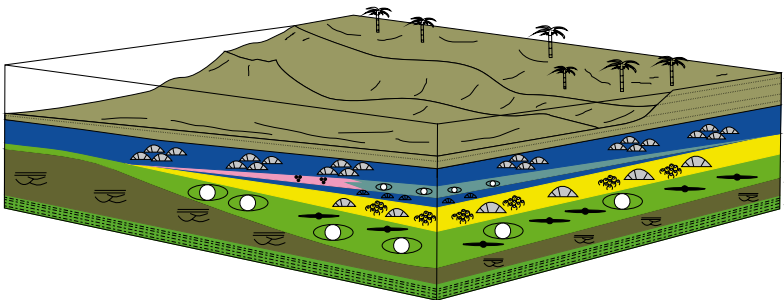
Fourth stage

- Depositional environment below the wave-base and separated from active deltaic systems.



Fifth stage

- Progradation of the deltaic system.
- Fall in sea level.
- Transition to non-marine sandstones.



- | | | | | | | | |
|--|--|--|---|--|-----------------------|--|--------|
| | Hummocky cross-stratification | | Coralline red algae | | Bryozoans | | Corals |
| | Progradation of deltaic system | | Discocyclus | | Nummulites | | |
| | Sandstone and marls | | Coralline red algal floatstone | | Nummulites floatstone | | |
| | Coral boundstone | | Bioclastic floatstone to rudstone with coral and bryozoans interbedded with marlstone | | | | |
| | Floatstone to rudstone with Discocyclus and Nummulites | | Sandstone and marls | | | | |
| | Cross bedded sandstone with microconglomerate intercalations | | | | | | |

FIGURE 7. Palaeoenvironmental reconstruction of the studied succession (not to scale).

in the transition area from the reef core to the marginal part, and the rudstone/bafflestone facies occurring in the marginal part of the reef core (Fig. 5A, B, C, D, G, H, I, J, K, L). Moreover, the scarce lateral continuity of the coral boundstone lithosomes suggests that they were constrained by the morphology of the underlying active deltaic deposits. Sometimes such environment was affected by episodic high-hydrodynamic pulses, allowing the skeletal sediments to be reworked. From this viewpoint, such coral lithosomes could be classified as sparse cluster-reefs *sensu* Riding (2002). Reefs on the delta fan system were submitted to important light fluctuations in mesophotic to aphotic zones and developed probably during periods with limited or without siliciclastic input. A similar situation was documented by Morsilli et al. (2011) in the coeval succession of Ainsa Basin (South Central Pyrenean zone). The two coral boundstone intervals are separated by *Nummulites* floatstone that passes laterally to coralline red algal floatstone. In particular, the thick- to thin-branching growth of coralline red algae and the abundance of *Gypsina moussaviani* with hooked morphologies suggests the occurrence of seagrass on the sea-bottom (Beavington-Penney et al., 2004; Sola et al., 2013). This would attest for a period with an unactive deltaic system and relatively low water turbidity (Fig. 7, stage 3). In contrast, the presence of several beds of microconglomerate toward the top of the sequence probably indicates the increase of fluvial input preceding the origin of the second coral buildup. Finally, the progradation of the deltaic system was related to a fall in sea level (Fig. 7, stage 5), as attested by the transition to the non-marine sandstones of the Sant Boi de Lluçanès and Artés Formations (Serra-Kiel et al., 2003a, b; Sanjuan et al., 2012).

DISCUSSION

The Priabonian coralgal buildup of the studied Orís sedimentary succession in the NE part of the Ebro Basin was related by Barnolas et al. (1988) and Serra-Kiel et al. (2003a) to the second Bartonian regressive cycle (Sant Martí Xic Formation). It consists of an alternation of offlap episodes, represented by deltaic deposits, and onlap episodes associated to marine deposits with larger foraminifera and coralgal facies. Costa et al. (2013), using integrated bio- and magnetostratigraphic data, re-assigned this cycle to the Priabonian.

The sedimentary succession is organized in two sedimentary sequences. The first is a transgressive sequence that starts with floatstone to rudstone with *Discocyclus* and *Nummulites* covered by coral boundstone, while the second, a regressive sequence, is characterized by *Nummulites* and coralline red algal floatstone overlain by the second coral boundstone

(second buildup). The cyclicity of the studied succession would be related both to local and global factors. Upper Eocene to lower Oligocene sedimentary successions follows worldwide (e.g. in European basins, Antarctica, East Asia and North America) a general climatic trend towards more arid climatic conditions (Sheldon and Retallack, 2004; Dupont-Nivet et al., 2008; Passchier et al., 2013; Utescher et al., 2015). Such a climatic trend is also recognized in the Ebro Basin and testified by a modification in the composition of plant biomes (Cavagnetto and Anadón, 1996; Bauer et al., 2016). However, the change in plant biomes did not correspond to a linear process but rather to short-term paleoclimatic fluctuations, in part related to orbital cyclicity influencing the precipitation rates (Postigo Mijarra et al., 2009; Tosal et al., 2019). The succession studied at Orís may be also influenced by similar short-term fluctuations.

During the Priabonian, the precipitation regime was relatively low and irregular, with a trend toward more arid conditions, mainly recorded in the coastal area and probably associated to oceanic regression. This lead finally to an increased continentalization of the Eurasian climate and a global temperature decrease (Postigo Mijarra et al., 2009). In Orís, this climate change might correspond to the replacement of *Discocyclus*-rich assemblages by *Nummulites*-dominated assemblages and is also testified by the decrease in carbonate content of the *Nummulites* floatstone in comparison with the second coral boundstone interval.

From the early Eocene climatic optimum (50–52Ma) until the start of the Oligocene (34Ma), a 17Myr-long abrupt fall in temperature occurred, culminating around 34Ma with the EOT events (Postigo Mijarra et al., 2009; Gandolfi et al., 2024). This temperature cooling was associated to an important glaciation (400kyr - Oi-1) and resulted in the development of the first Cenozoic Antarctic ice cap (Miller et al., 1991; Zachos et al., 2001). In the Ebro Basin important palynological changes were recorded at the boundary between Bartonian and Priabonian. Mangroves disappeared and plant associations shifted to biomes better adapted to drier climates, including savannahs (Cavagnetto and Anadón, 1996; Tosal et al., 2019). However, despite this climatic trend, several marine and continental palaeotropical species survived better in the Iberian Peninsula than in other areas of Europe, suggesting that the peninsula may have acted as a biogeographic refuge thanks to its southern palaeolatitude, to its varied orography and microclimatic diversity (Tosal et al., 2024, and references therein). Also, the influence of the Tethyan and Atlantic oceans, providing constant humidity across several peninsular areas, must be considered as a significant factor of temperature attenuation (Postigo Mijarra et al., 2009).

This climatic situation may have also affected the development of the coral buildups studied. The architecture of the coralgal buildups suggests adaptation to low light intensity, showing coral colonies growing wider than higher in order to increase the surface exposed to sunlight. Alternatively, they grew on top of pseudocolonial forms (phaceloid shapes) to avoid being covered by sediment, with platy corals serving as ground for more complex colonies, such as rare domes (Fig. 6A). Unstable environments resulted in low coral biodiversity with *Cereiphylla* sp., *Ellipsocoenia* sp., *Goniopora* sp., *Caulastrea* sp., and *Actinacis* sp. being the main components.

In this view, the coralgal buildups studied here represent a good example of reefs developed under turbid water conditions in the sense of Sanders and Baron-Szabo (2005). These reefs were influenced by discontinuous sediment supply associated to climate oscillations, unstable precipitation rate (e.g. Gómez-Paccard et al., 2012) and possibly also active tectonics, related to the contemporary uplift of the western Pyrenees and the nearby Bellmunt anticline (Vilà-Vinyet, 2010) (Fig. 1).

Similar environmental scenarios were described in other localities. In the Upper Austrian Alpine foreland basin, Rasser (2009) reported coeval deposits to the Orís buildups with corals sharing similar patterns of poor diversity and growth morphology. Coralline red algae lithofacies attested for an environment mainly controlled by good light conditions and associated to inactive deltaic systems covered by seagrass (Nebelsick et al., 2005). The adaptation of corals to similar environments was also described by Bosellini and Trevisani (1992), Bosellini (1998), Bosellini and Papazzoni (2003) in the succession of the Nago Limestone (Venetian region, North Italy) and by Morsilli et al. (2011) in coeval examples of the Ainsa Basin (southern central Pyrenees). The coralgal buildups of the Orís section show limited lateral extension and thickness when compared with the coeval deposits of the Ainsa Basin. This space limitation could result from the growth of corals upon a small, pre-existing deltaic lobe.

Further examples of corals adapted to similar environmental conditions and palaeotopographic constraints were described in non-coeval records. Thus, during the Late Oligocene Warming Event in the Piedmont Basin (NW Italy) Bosellini et al. (2024) describe a deltaic system developed in a narrow palaeovalley, where discontinuous coral buildups grew in the pro-delta under mesophotic conditions. These coral buildups grew during periods of inactive deltaic systems or thanks to a by-pass of the fluvial sediment.

Another important factor to be considered to interpret correctly the growth of coral buildups is the Cenozoic

change in marine water circulation proposed by Pomar et al. (2017). This was related to new thermal gradients that induced the formation of waves or currents at different depths and latitudes. The increase of such currents and waves changed the nutrient supply, feeding in particular the plankton catchers, such as corals, and limiting the distribution of larger benthic foraminifera. Although such currents might not have reached the easternmost Ebro basin, the fact that occurrence of larger benthic foraminifera (*Discocyclina*/*Nummulites*) in the Orís section was reduced in the areas where the succession of coral boundstone was developed, suggest similar patterns to those described by Pomar et al. (2017).

All these considerations suggest that the studied sedimentary succession at Orís was influenced by simultaneous processes, such as light fluctuation, high sedimentary rates and increase in nutrient supply, leading to mesotrophic conditions. In particular the deposition of floatstone to rudstone with *Discocyclina* and *Nummulites*, suggests a period of stronger activity of the deltaic system associated to more humid conditions, while the deposition of the *Nummulites* floatstone and coralline red algal floatstone, suggest deltaic systems with variable water turbidity and developed under drier climatic conditions. This view is supported by the absence of *Discocyclina*. Coral boundstone displays lens-shaped bioherms, with geometries being possibly controlled by the pre-existing deltaic morphology and nutrient distribution, rather than by climatic constraints (e.g. Pomar et al., 2017). Nutrient distribution was related to marine currents, hydrodynamic conditions and the palaeotopography, the latter being strictly linked to the uplift of the Catalan Coastal Range (Vergès et al., 2002). The interaction of the local and global factors reported above reveal the complexity of sedimentary successions in a shallow water setting and document the resilience of Eocene corals to environmental change.

CONCLUSIONS

The sedimentary successions in both continental and marine environments are a valuable tool to recognize how biotas responded to global and local environmental factors with varying adaptive strategies. In particular, different lithofacies and biofacies are directly indicative of the environmental conditions preserved within the sedimentary record. The upper Eocene Sant Martí Xic Formation and its sedimentary succession studied at Orís, (Vic, SE Ebro basin, Spain), is characterized by different depositional stages.

The first stage, represented by the deposition of the rudstone to floatstone with *Discocyclina* and *Nummulites*,

testifies for an environment below the fair-weather wave-base level, related to the middle ramp. This environment, with low light intensity, was associated to turbid water and humid climate conditions. The second stage, that includes the first coral boundstone interval, reveals instead a low energy environment below the fair-weather wave-base characterized by low sediment supply due to the inactive deltaic system or to deposition in an area away from deltaic influence. The third stage was instead associated to two different environmental settings associated to dry climate conditions. The first one was represented by *Nummulites* floatstone and suggests an environment affected by the active deltaic system with low light intensities. In contrast, the second environmental setting reveals low water turbidity in a period when the deltaic system was not active (coralline red algae floatstone). Microconglomerates overlaying the third stage lithofacies suggest the onset of the fluvial input and the progradation of the deltaic system, stopped during the development of the second coral boundstone layer (fourth stage). This stage displays similar conditions to those described by the second stage. Finally, a fall in sea level determined the transition to the continental sandstones of the Sant Boi and Artés formations (fifth stage).

The two coralgal buildups interdigitated with deltaic system deposits studied at Orís, were influenced two main large-scale factors, firstly the tectonic activity, related to the uplift of the western Pyrenees, and secondly the climatic fluctuations with discontinuous sediment supply mainly related to precipitation rate. The cyclicity in the appearance of these buildups is linked to short-term paleoclimatic fluctuations during the Priabonian, a period characterized by low and irregular precipitation, with a trend towards increasingly arid conditions. Despite these environmental shifts the studied buildups represent the resilience of Eocene corals to both climatic and local environmental changes.

ACKNOWLEDGMENTS

This study is a contribution to the projects BIOGEOMODELS (PID2020-113912GB-I00), funded by MCIN/AEI/10.13039/501100011033 and 2021SGR-00349 *Geologia Sedimentaria* founded by AGAUR, Generalitat de Catalunya. We acknowledge the assistance of Johannes Pignatti in the identification of foraminifera, and Josep Serra-Kiel, Flavio Priore, Antonio Mancini and Jordi Vilà for their assistance in the field. We are grateful to the editor C. Martín-Closas and two anonymous reviewers for their useful comments and constructive criticisms that substantially improved the quality of the manuscript. The authors dedicate this study to Emeritus Prof. Ramon Salas, who first studied into detail the coralgal buildups of the eastern Ebro Basin, in the area of Igualada.

REFERENCES

- Álvarez, G., Busquets, P., Taberner, C., Urquiola, M.M., 1994. Facies architecture and coral distribution in a mid Eocene reef tract, South Pyrenean Foreland Basin (NE Spain). *Cour. Forsch.Inst. Senckenberg [Courier Forschungsinstitut Senckenberg]*, 172, 249-259.
- Álvarez, G., Bosence, D., Busquets, P., Darrell, J.G., Franquès, J., Gili, E., Pisera, A., Reguant, S., Rosen, B.R., Salas, R., Serra-Kiel, J., Skelton, P.W., Taberner, C., Travé, A., Valdeperas, E.X., 1995. Bioconstructions of the Eocene South Pyrenean Foreland Basin (Vic and Igualada Areas) and of the Upper Cretaceous South Central Pyrenees (Tresp area). Madrid, VII Int. Symp. on Fossil Cnidaria and Porifera (field trip c), 68pp.
- Álvarez, G., Busquets, P., Franquès, J., 1999. Diversidad, composición y estructura de un arrecife coralino del Bartonense de la Cuenca del Ebro (extremo nororiental). *Temas Geológico-Mineros ITGE*, 26, 491-494.
- Barnolas, A., 1992. Evolución sedimentaria de la Cuenca Surpirenaica Oriental durante el Eoceno. *Acta Geologica Hispanica*, 27, 15-31.
- Barnolas, A., Busquets, P., Serra-Kiel, J., 1981. Características sedimentológicas de la terminación del ciclo marino del Eoceno superior en el sector oriental de la depresión del Ebro (Catalunya N-E de España). *Acta Geologica Hispanica*, 16, 215-221.
- Barnolas, A., Reguant, S., Busquets, P., Colombo, E., Vilaplana, M., Serra-Kiel, J., 1983. Mapa geológico de España. Scale 1:50.000, 2nd series, No. 332, Vic. Madrid, Instituto Geológico y Minero de España (IGME), Servicio de Publicaciones del Ministerio de Industria, 23pp., 1 fold map.
- Barnolas, A., Samsó, J., Serra-Kiel, J., Tosquella, J., 1988. Estructura interna del sistema deposicional de Sant Martí Xic. *Geogaceta*, 5, 69-71.
- Bassi, D., 1998. Coralline Algal Facies and their paleoenvironments in the Late Eocene of Northern Italy (Calcare di Nago, Trento). *Facies*, 39, 179-202.
- Bauer, M.P., Tselioudis, G., Rossow, W.B., 2016. A new climatology for investigating storm influences in and on the extratropics. *J. Appl. Meteorol. Climatol.*, 55(5), 1287-1303. DOI: 10.1175/JAMC-D-15-0245.1
- Beavington-Penney, S.J., Racey, A., 2004. Ecology of extant nummulitid and other larger benthic foraminifera: applications in palaeoenvironmental analysis. *Earth Sci Rev.* 67, 219-265. DOI: <https://doi.org/10.1016/j.earscirev.2004.02.005>
- Beavington-Penney, S.J., Wright, P.V., Woelkerling, W.J., 2004. Recognising macrophyte-vegetated environments in the rock record: a new criterion using 'hooked' forms of crustose coralline red algae. *Sediment Geol.* 166, 1-9. DOI: <http://dx.doi.org/10.1016/j.sedgeo.2003.11.022>
- Beger, M., Sommer, B., Harrison, P.L., Smith, S.D.A., Pandolfi, J.M., 2014. Conserving potential coral reef refuges at high latitudes. *Diversity and distribution*, 20(3), 245-257. DOI: <https://doi.org/10.1111/ddi.12140>

- Bosellini, FR., 1998. Diversity, Composition and structure of Late Eocene shelf-edge coral associations (Nago Limestone, Northern Italy). *Facies*, 39, 203-226. DOI: <http://dx.doi.org/10.1007/BF02537017>
- Bosellini, F., Trevisani, E., 1992. Coral facies and cyclicity in the Castelmomberto Limestone (Early Oligocene, Eastern Lessini Mountains, Northern Italy). *Rivista Italiana di Paleontologia e Stratigrafia*, 98(3), 339-352.
- Bosellini, FR., Papazzoni, C.A., 2003. Palaeoecological significance of coral-encrusting foraminiferan associations: a case-study from the upper Eocene of northern Italy. *Acta Palaeontol Pol*, 48, 279-292.
- Bosellini, FR., Vescogni, A., Briguglio, A., Piazza, M., Papazzoni, C., Silvestri, G., Morsilli, M., 2024. Resilient coral reef ecosystems: The case study of turbid-mesophotic coral buildups during the Late Oligocene Warming Event (Tertiary Piedmont Basin, NW Italy). *Palaeogeography, Palaeoclimatology, Palaeoecology*, 649, 1-19. DOI: [10.1016/j.palaeo.2024.112330](https://doi.org/10.1016/j.palaeo.2024.112330)
- Cabello, P., Falivene, O., López-Blanco, M., Howell, J., Arbués, P., Ramos, E., 2010. Modelling facies belt distribution in fan deltas coupling sequence stratigraphy and geostatistics: The Eocene Sant Llorenç del Munt example (Ebro foreland basin, NE Spain). *Mar Petrol Geol*, 27, 254-272.
- Cavagnetto, C., Anadón, P., 1996. Preliminary palynological data on floristic and climatic changes during the Middle Eocene-Early Oligocene of the eastern Ebro Basin, northeast Spain. *Review of Palaeobotany and Palynology*, 92(3-4), 281-305. DOI: [https://doi.org/10.1016/0034-6667\(95\)00096-8](https://doi.org/10.1016/0034-6667(95)00096-8)
- Coletti, G., Mariani, L., Garzanti, E., Consani, S., Bosio, G., Vezzoli, G., Hu, X., Basso, D., 2021. Skeletal assemblages and terrigenous input in the Eocene carbonate systems of the Nummulitic Limestone (NW Europe). *Sedimentary Geology*, 425, 106005. DOI: <https://doi.org/10.1016/j.sedgeo.2021.106005>
- Costa, E., Garcés, M., López-Blanco, M., Serra-Kiel, J., Bernalda, G., Cabrera, L., Beamud, E., 2013. Bartonian-Priabonian marine record of the eastern South Pyrenean foreland basin (NE Spain): a new calibration of the larger foraminifers and calcareous nannofossil biozonation. *Geologica Acta*, 11, 177-193.
- Dunham, R.J., 1962. Classification of carbonate rocks according to depositional texture. In: Ham, W.E. (ed.). *Classification of Carbonate Rocks*. Mem Am Assoc Pet Geol, 1, 108-121.
- Dupont-Nivet, G., Hoorn, C., Konert, M., 2008. Tibetan uplift prior to the Eocene-Oligocene climate transition: Evidence from pollen analysis of the Xining Basin. *Geology*, 36(12), 987-990. DOI: <https://doi.org/10.1130/G25063A.1>
- Ferrández-Cañadell, C., Serra-Kiel, J., 1992. Morphostructure and paleobiology of *Discocyclus* Gümbel, 1870. *J Foram Res*, 22(2), 147-165.
- Ferrer, J., 1971. El Paleoceno y Eoceno del borde suroccidental de la Depresión del Ebro (Cataluña). *Mémoires suisses de Paléontologie*, 90, 70pp.
- Ferrer, J., Rosell, J., Reguant, S., 1968. Síntesis litoestratigráfica del Paleógeno del borde oriental de la depresión del Ebro. *Acta Geol Hispanica*, 3, 54-56.
- Gandolfi, A., Giraldo-Gómez, VM., Luciani, V., Piazza, M., Brombin, V., Crobu, S., Papazzoni, C.A., Pignatti, J., Briguglio, A., 2024. Unraveling ecological signals related to the MECO onset through planktic and benthic foraminiferal records along a mixed carbonate-siliciclastic shallow-water succession. *Marine Micropaleontology*, 190, 102388. DOI: <https://doi.org/10.1016/j.marmicro.2024.102388>
- Garcés, M., López-Blanco, M., Valero, L., Beamud, E., Muñoz, J.A., Oliva-Urcia, B., Vinyoles, A., Arbués, P., Cabello, P., Cabrera, L., 2020. Paleogeographic and sedimentary evolution of the south-Pyrenean foreland basin. *Marine and Petroleum Geology*, 113, 104105. DOI: <https://doi.org/10.1016/j.marpetgeo.2019.104105>
- Gómez-Paccard, M., López-Blanco, M., Costa, E., Garcés, M., Beamud, E., Larrasoña, J.C., 2012. Tectonic and climatic controls on the sequential arrangement of an alluvial fan/fan-delta complex (Montserrat, Eocene, Ebro Basin, NE Spain). *Basin Res*, 24, 437-455.
- Insalaco, E., 1998. The descriptive nomenclature and classification of growth fabrics in fossil scleractinian reefs. *Sediment Geol*, 118, 159-186.
- Lesser, M.P., Slattery, M., Leichter, J.J., 2009. Ecology of mesophotic coral reefs. *J Exp Mar Biol Ecol*, 375, 1-8.
- Lokier, S.W., Wilson, M.E.J., Burton, L.M., 2009. Marine biota response to clastic influx: A quantitative approach. *Palaeogeogr Palaeoclimatol Palaeoecol*, 281, 25-42.
- López-Blanco, M., Marzo, M., Piña, J., 2000. Transgressive-regressive sequence hierarchy of foreland, fan-delta clastic wedges (Montserrat and Sant Llorenç del Munt, Middle Eocene, Ebro Basin, NE Spain). *Sediment Geol*, 138, 41-69.
- Mariani, L., Coletti, G., Bosio, G., Mateu Vicens, G., Ali, M., Cavallo, A., Mittempergher, S., Malinverno, E., 2024. Tectonically-controlled biofacies distribution in the Eocene Foraminiferal Limestone (Pag, Croatia): A quantitative-based palaeontological analysis. *Sedimentary Geology*, 472, 106743. DOI: <https://doi.org/10.1016/j.sedgeo.2024.106743>
- Miller, K.G., Wright, J.D., Fairbanks, R.G., 1991. Unlocking the ice house: Oligocene-Miocene oxygen isotopes, eustasy, and margin erosion. *Journal of Geophysical Research*, 96(6), 829-848.
- Morgan, K.M., Perry, C.T., Johnson, J.A., Smithers, S.G., 2017. Nearshore turbid-zone corals exhibit high bleaching tolerance on the great barrier reef following the 2016 ocean warming event. *Front. Mar. Sci.* 4:224. DOI: [10.3389/fmars.2017.00224](https://doi.org/10.3389/fmars.2017.00224)
- Morsilli, M., Bosellini, FR., Pomar, L., Hallock, P., Aurell, M., Papazzoni, C.A., 2011. Mesophotic coral buildups in a prodelta setting (Late Eocene southern Pyrenees, Spain): a mixed carbonate-silicoclastic system. *Sedimentology*, 59, 766-794.
- Muñoz, J.A., Martínez, A., Vergès, J., 1986. Thrust sequences in the eastern Spanish Pyrenees. *Jour Structural Geol*, 8, 399-405.

- Nebelsick, J.H., Rasser, M.W., Bassi, D., 2005. Facies dynamics in Eocene to Oligocene circumalpine carbonates. *Facies*, 51, 197-216.
- Passchier, S., Falk, C.J., Florindo, F., 2013. Orbitally paced shifts in the particle size of Antarctic continental shelf sediments in response to ice dynamics during the Miocene climatic optimum. *Geosphere*, 9, 54-62. DOI: <https://doi.org/10.1130/GES00840.1>
- Perry, C.T., Smithers, S.G., 2006. Taphonomic signatures of turbid-zone reef development: examples from Paluma Shoals and Luggar Shoal, inshore central Great Barrier Reef, Australia. *Palaeogeogr Palaeoclimatol Palaeoecol*, 242, 1-20.
- Pochon, X., Pawlowski, J., 2006. Evolution of the soritids-Symbiodinium symbiosis. *Symbiosis*, 42, 77-88.
- Pomar, L., Baceta, J.I., Hallock, P., Mateu-Vicens, G., Basso, D., 2017. Reef building and carbonate production modes in the west-central Tethys during the Cenozoic. *Marine and Petroleum Geology*, 83, 261-304. DOI: <https://doi.org/10.1016/j.marpetgeo.2017.03.015>
- Postigo Mijarra, J.M., Barrón, E., Manzaneque, F.G., Morla, C., 2009. Floristic changes in the Iberian Peninsula and Balearic Islands (south-west Europe) during the Cenozoic. *J. Biogeogr.*, 36, 2025-2043.
- Rasser, M.W., 2009. Coralline red algal limestones of the late Eocene alpine Foreland Basin in Upper Austria: Component analysis, facies and paleocology. *Facies*, 42, 59-92.
- Riding, R., 2002. Structure and composition of organic reefs and carbonate mud mounds: concepts and categories. *Earth Sci Rev*, 58, 163-231.
- Reuter, M., Bosellini, F.R., Budd, A.F., Ćorić, S., Piller, W.E., Harzhauser, M., 2019. High coral reef connectivity across the Indian Ocean is revealed 6–7 Ma ago by a turbid-water scleractinian assemblage from Tanzania (Eastern Africa). *Coral Reefs*, 38, 1023-1037. DOI: <https://doi.org/10.1007/s00338-019-01830-8>
- Romero, J., Caus, E., Rosell, J., 2002. A model for the palaeoenvironmental distribution of larger foraminifera based on late Middle Eocene deposits on the margin of the South Pyrenean basin (NE Spain). *Palaeogeogr Palaeoclimatol Palaeoecol*, 179, 43-56.
- Rosedy, A., Ives, I., Waheed, Z., Hussein, M.A.L., Sosdian, S., Johnson, K., Santodomingo, N., 2023. Turbid reefs experience lower coral bleaching effects in NE Borneo (Sabah, Malaysia). *Regional Studies in Marine Science*, 68, 103268. DOI: <https://doi.org/10.1016/j.rsma.2023.103268>
- Salas, R., 1979. El sistema arrecifal del Eoceno Superior de la Cuenca de Igualada, Barcelona. Master Degree Thesis. Barcelona, University of Barcelona, 196pp.
- Sanders, D., Baron-Szabo, R.C., 2005. Scleractinian assemblages under sediment input: their characteristics and relation to the nutrient input concept. *Palaeogeogr Palaeoclimatol Palaeoecol*, 216, 139-181.
- Sanjuan, J., Martín-Closas, C., 2012. Charophyte palaeoecology in the Upper Eocene of the Eastern Ebro basin (Catalonia, Spain). *Biostratigraphic implications*. *Palaeogeography, Palaeoclimatology, Palaeoecology*, 365-366, 247-262.
- Sanjuan, J., Martín-Closas, C., Serra-Kiel, J., Gallardo, H., 2012. Stratigraphy and biostratigraphy (charophytes) of the marine-terrestrial transition in the Upper Eocene of the NE Ebro Basin (Catalonia, Spain). *Geologica Acta*, 10, 19-31.
- Santisteban, C., Taberner, C., 1988. Sedimentary models of siliciclastic deposits and coral reef interactions. In: Doyle L.J., Roberts, H.H. (eds.). *Carbonate-clastic transitions*. *Dev Sedimentol*, 42, 35-76.
- Santodomingo, N., Novak, V., Pretković, V., Marshall, N., Di Martino, E., Lo Giudice Capelli, E., Rösler, A., Reich, S., Braga, J.C., Renema, W., Johnson, K.G., 2015. A diverse patch reef from turbid habitats in the Middle Miocene (East Kalimantan, Indonesia). *Palaaios*, 30, 128-149.
- Santodomingo, N., Renema, W., Johnson, K.G., 2016. Understanding the murky history of the Coral Triangle: Miocene corals and reef habitats in East Kalimantan (Indonesia). *Coral Reefs*, 35, 765-781. DOI: <https://doi.org/10.1007/s00338-016-1427-y>
- Saula, E., Picart, J., Mató, E., Llenas, M., Losantos, M., Berástegui, X., Agustí, J., 1994. Evolución geodinámica de la fosa del Empordà y las Sierras Transversales. *Acta Geologica Hispanica*, 29, 55-75.
- Serra-Kiel, J., Hottinger, L., Caus, E., Drobne, K., Ferràndez, C., Jauhri, A.K., Less, G., Pavlovec, R., Pignatti, J., Samsó J.M., Schaub, H., Sirel, E., Strugo, A., Tambareau, Y., Tosquella, J., Zakrevskaya, E., 1998. Larger foraminiferal biostratigraphy of the Tethyan Paleocene and Eocene. *Bull Geol Soc France*, 169, 281-299.
- Serra-Kiel, J., Mató, E., Saula, E., Travé, A., Ferràndez-Cañadell, C., Busquets, P., Samsó, J.M., Tosquella, J., Barnolas, A., Álvarez-Pérez, G., Franquès, J., Romero, J., 2003a. An inventory of marine and transitional Middle/Upper Eocene deposits of the southeastern Pyrenean foreland basin (NE Spain). *Geologica Acta*, 1, 201-229.
- Serra-Kiel, J., Mató, E., Saula, E., Travé, A., Ferràndez-Cañadell, C., Busquets, P., Tosquella, J., Vergès, J., 2003b. Marine and transitional Middle/Upper Eocene units of the southeastern Pyrenean foreland basin (NE Spain). *Geologica Acta*, 1, 177-200.
- Sheldon, N.D., Retallack, G.J., 2004. Regional paleoprecipitation records from the late Eocene and Oligocene of North America. *The Journal of Geology*, 112, 487-494.
- Sola, F., Braga, J.C., Aguirre, J., 2013. Hooked and tubular coralline algae indicate seagrass beds associated to Mediterranean Messinian reefs (Poniente Basin, Almería, SE Spain). *Palaeogeogr Palaeoclimatol Palaeoecol*, 374, 218-229.
- Sully, S., van Woesik, R., 2020. Turbid reefs moderate coral bleaching under climate-related temperature stress. *Global change Biology*, 26(3), 1367-1373. DOI: <https://doi.org/10.1111/gcb.14948>
- Taberner, C., Bosence, D.W.J., 1995. An Eocene biotrital mudmound from the southern Pyrenean foreland basin, Spain: an ancient analogue for Florida Bay mounds? In: Monty, C.L.V., Bosence, D.W.J., Bridges, P.H., Pratt, B.R. (eds.). *Carbonate Mud Mounds – Their Origin and Evolution*. IAS 23 (Special Publication), 423-437.

- Tomassetti, L., Bosellini, F., Brandano, M., 2013. Growth and demise of a Burdigalian coral bioconstruction on a granite rocky substrate (Bonifacio Basin, South Corsica). *Facies*, 59(4), 703-716. DOI: 10.1007/s10347-012-0341-1
- Tosal, A., Valero, L., Sanjuan, J., Martín-Closas, C., 2019. Influence of short- and long-term climatic cycles on floristic change across the Eocene–Oligocene boundary in the Ebro Basin Catalonia, Spain). *Comptes Rendus Palevol*, 18, 925-947.
- Tosal, A., Vicente, A., Denk, T. 2024. Cenozoic Ampelopsis and Nekemias leaves (Vitaceae, Ampelopsidae) from Eurasia: paleobiogeographic and paleoclimatic implications. *Jornal of Systematics and Evolution*. doi: 10.1111/jse.13126
- Travé, A., Serra-Kiel, J., Zamarreño, I., 1996. Paleoeological interpretation of transitional environments in Eocene carbonates (NE Spain). *Palaios*, 11, 141-160.
- Utescher, T., Bondarenko, O.V., Mosbrugger, V., 2015. The Cenozoic Cooling – continental signals from the Atlantic and Pacific side of Eurasia. *Earth and Planetary Science Letters*, 415, 121-133. DOI: <https://doi.org/10.1016/j.epsl.2015.01.019>
- Vergès, J., Fernández, M., Martínez, A., 2002. The Pyrenean orogen: pre-, syn-, and post- collisional evolution. In: Rosenbaum, G., Lister, G., (eds.). *Reconstruction of the evolution of the Alpine-Himalayan Orogen*. *J Virtual Explorer* 8, 55-74. DOI: 10.3809/jvirtex.2002.00058
- Vilà-Vinyet, J., 2010. Delimitació de la sedimentació sintectònica associada a l'aixecament de l'Anticlinal de Bellmunt (Eocè superior, Bartonian-Priabonian, NE de la Conca de l'Ebre). Master Degree. Universitat de Barcelona.
- Wilson, M.E.J., Lokier, S.W., 2002. Siliciclastic and volcanoclastic influences on equatorial carbonates: insights from the Neogene of Indonesia. *Sedimentology*, 49, 583-601.
- Woolfe, K.J., Larcombe, P., 1998. Terrigenous sediment accumulation as a regional control on the distribution of reef carbonates. In: Camoin, G.F., Davies, P.J., (eds.). *Reefs and Carbonate Platforms in the Pacific and Indian Oceans*. IAS, 25 (Special Publication), 295-310.
- Zachos, J., Pagani, M., Sloan, L., Thomas, E., Billups, K., 2001. Trends, Rhythms, and Aberrations in Global Climate 65 Ma to Present. *Science*, 292(5517), 686-693. DOI: 10.1126/science.1059412
- Zweifler (Zvifler), A., O'Leary, M., Morgan, K., Browne, N.K., 2021. Turbid Coral Reefs: Past, Present and Future—A Review. *Diversity*, 13(6), 251. DOI: <https://doi.org/10.3390/d13060251>

Manuscript received October 2024;

revision accepted May 2025;

published Online August 2025.